Journal of Medicinal and Nanomaterials Chemistry 1 (2024) 64-80

SPC

Journal of Medicinal and Nanomaterials Chemistry

Journal homepage: https://jmnc.samipubco.com/

Original Resesrch Article

Quantum chemical and molecular docking studies of luteolin and naringerin found in tigernut: A study of their anti-cancer properties

Deborah Alahira [1], John Paul Shinggu [2, 3]*, Bulus Bako [2, 3]

[1] *Department of Food Science and Technology, Federal University Wukari, Taraba State, Nigeria*
[2] *Computational Astrochemistry and Bio-Simulation Research Group, Federal University Wukari, Taraba State, Nigeria*
[3] *Department of Chemical Sciences, Federal University Wukari, Taraba State, Nigeria*

ARTICLE INFORMATION

Submitted: 2024-02-25
Revised: 2024-03-26
Accepted: 2024-04-14

Manuscript ID: JMNC-2403-1023
Checked for Plagiarism: **Yes**
Language Editor Checked: **Yes**
DOI: 10.48309/JMNC.2024.1.6

KEYWORDS

Molecular docking
Naringerin
Luteolin
Cancer
Quantum chemical studies
Tigernut

ABSTRACT

In recent years, the exploration of natural compounds from plants has gained traction as researchers seek alternatives to conventional cancer therapies. Luteolin and Naringenin, identified in Tigernuts, have been of particular interest due to their established anti-cancer potential within the broader class of flavonoids. Against the backdrop of rising global cancer prevalence, this study explores the potential of plant-derived compounds as alternatives or complementary therapies. This study investigates the anti-cancer properties of Luteolin and Naringenin, prominent flavonoids found in Tigernuts (Cyperus esculentus L.). A computational modeling method known as molecular docking was employed to predict the preferred orientations of Luteolin and Naringenin when forming stable complexes with cancer-related molecular targets. In addition, density functional theory (DFT) was utilized to calculate the electronic structure of these compounds, providing insights into their stability and reactivity. As conventional chemotherapeutic approaches face limitations, this contributes to the ongoing quest for efficient and side effect-minimized cancer treatments. The results of this study showed that naringerin and luteolin found in tigernut has great potential to be used in the fight against cancer, showcasing the potential of natural compounds from Tigernuts in contemporary cancer research and drug development.

Corresponding author, email: johnshinggu@gmail.com (J.P. Shinggu).

Graphical Abstract

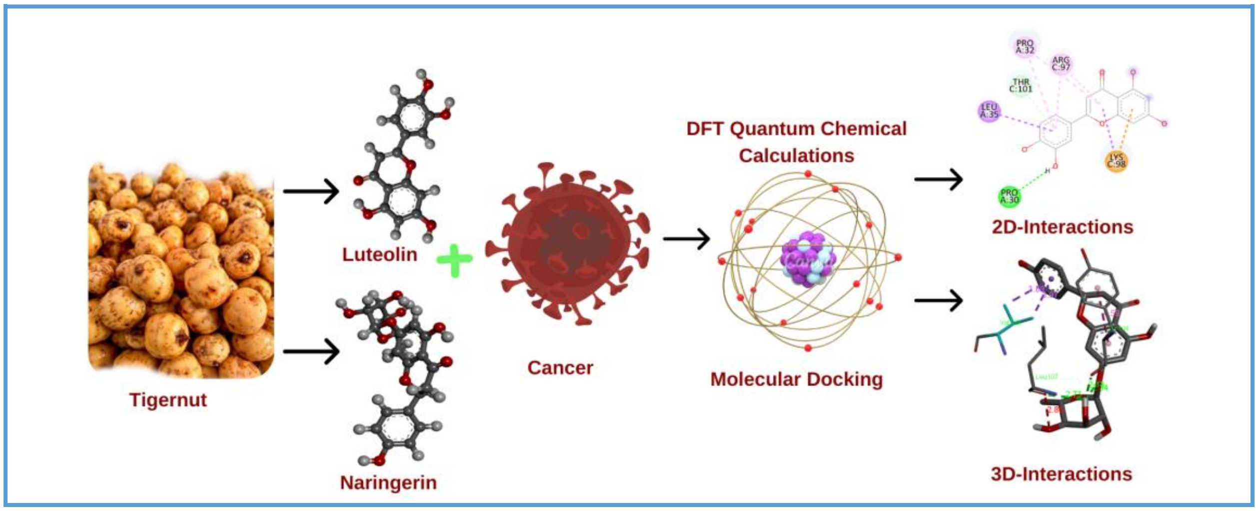

Introduction

In recent years, the exploration of natural compounds from plants has gained traction as researchers seek alternatives to conventional cancer therapies. Luteolin and Naringenin, identified in Tigernuts, have been of particular interest due to their established anti-cancer potential within the broader class of flavonoids [1,2]. These compounds have demonstrated a range of biological activities, including anti-inflammatory, antioxidant, and anti-proliferative effects, making them promising candidates for further investigation in the context of cancer treatment [3,39].

Cancer is a pervasive global health concern and continues to exert a significant toll on human lives, with millions of new cases and deaths reported annually [4-6]. Seeking innovative and effective strategies for cancer prevention and treatment has become paramount in contemporary research. This study describes the potential anti-cancer properties of Luteolin and Naringenin, two bioactive compounds abundantly present in tigernuts (Cyperus esculentus L.), commonly known as "subterranean walnuts" [7,8].

Tigernuts were historically confined to the Mediterranean Region have now become a globally cultivated crop, recognized for their prolific output and versatile applications [9]. In Nigeria, these tuberous plants are cultivated both as a weed and a valuable crop due to their edible tubers [10]. The rich phytochemical profile of tigernuts includes flavonoids, organic acids, alkaloids, glycosides, monounsaturated fatty acids, tannins, phytates, and oils, with tigernut oil sharing a nutritional profile comparable to olive oil [11-13].

Given the rising cancer prevalence worldwide, the exploration of plant-derived anti-cancerous agents has gained considerable attention [14]. The compounds of interest, Luteolin and Naringenin, fall under the category of flavonoids and their derivatives, known for their potential anti-cancer properties [15,17]. This clearly means that a computational approach to solve the health challenge of cancer using computational tools is highly sought after. Bioactive compounds, as the secondary metabolites of foods, offer not only basic nutritional values, but also health protection, making them promising candidates for cancer prevention and treatment [16,40,45].

Molecular docking, a computational modeling method, emerges as a promising avenue for cancer cell targeting through drug design and discovery programs [18-20]. This method predicts the preferred orientation of molecules when forming stable complexes, presenting a cost-effective and time-saving alternative to conventional approaches in cancer treatment. In addition, density functional theory (DFT), a quantum-mechanical method, plays a pivotal role in calculating the electronic structure of molecules, paving the way for a deeper understanding of their interactions and potential applications in cancer research [21-24].

As conventional chemotherapeutic approaches face limitations, the quest for novel and efficient drugs with minimal side effects intensifies [25,26]. This study aims to contribute to this endeavor by investigating the anti-cancer properties of luteolin and naringenin through quantum chemical and molecular docking studies which has been neglected in various anti-cancer studies [27]. By elucidating the molecular interactions and electronic structures, we aim to provide insights that could pave the way for the development of targeted and effective therapies in the fight against cancer. This showcases the drawbacks of other researches.

Computational methods

The computational methodology employed in this research harnessed the robust capabilities of the GAUSSIAN 09 suite of programs [28,29]. To conduct quantum chemical calculations, advanced computational methods, specifically the density functional theory (DFT), were utilized. The optimization and frequency calculations of Luteolin and Naringerin were executed employing the widely recognized B3LYP functional and the 6-311*G (d, p) basis set [30,41]. This specific combination of functional and basis set is known for providing accurate and comprehensive insights into the energetics, geometry, and electronic structure of molecules, thus affording a quantum-level understanding of the molecular properties.

Through DFT calculations such as the time dependent density functional theory (TD-DFT) calculations, a spectrum of molecular properties, including UV-Vis absorption, IR vibrational frequencies, and NMR chemical shifts, were accurately predicted [31,36]. The chosen methodology allows for a thorough exploration of electronic and vibrational transitions, enhancing our ability to interpret and comprehend the intricate molecular characteristics of Luteolin and Naringerin [43,44]. Notably, the precision of these calculations is crucial in providing reliable data for the subsequent analysis and interpretation of the results, ensuring the robustness and validity of the findings in the context of the specified quantum chemical framework [42].

Molecular docking protocol

Molecular docking simulation is a method of computational simulation which studies the interactions between smaller molecules called ligands and macromolecules called proteins [46]. In this study, we conducted a molecular docking analysis to investigate the potential interactions of Naringenin and Luteolin with the MDM2 protein (PDB ID: 4ZFI). Both Naringenin and Luteolin were chosen as ligands due to their relevance and potential therapeutic implications. The ligands' 3D structures were optimized, and a grid around the active site of the MDM2 protein was defined for docking simulations [32]. Multiple docking runs were performed using AutoDock Vina, and the resulting complexes were analyzed for binding affinities and key molecular interactions. The study aimed to elucidate the binding modes and potential therapeutic impact of Naringenin and Luteolin on the MDM2 protein, contributing to a better understanding of their pharmacological relevance in anti-cancer studies [33]. The preparation of ligands and the MDM2 protein for molecular docking simulations was carried out using AutoDock Tools software. The molecular docking analysis, conducted with AutoDock Vina through command prompt execution, aimed to explore the interactions between the ligands (Naringenin and Luteolin) and the MDM2 protein (PDB ID: 4ZFI) [33].

Subsequently, the resulting docked complex underwent comprehensive analysis in both 2D and 3D formats. Discovery Studio was employed for the visualization of 2D structures, while 3D visualization was facilitated using the same software. The 3D structures of the MDM2 protein (4ZFI) were retrieved from the Research Collaborator for Structural Bioinformatics (RCSB) protein data bank, offering insights into the structural characteristics of this crucial protein involved in various cellular processes, including its interaction with ligands such as Naringenin and Luteolin [34,38].

Drug-likeness, pharmacokinetic and pharmacodynamic studies

In examining the pharmacokinetic and pharmacodynamic profiles of Naringenin and Luteolin, we adopted a comprehensive approach. The pharmacokinetic analysis involved scrutinizing the absorption, distribution, metabolism, excretion, and toxicity (ADMET) aspects [35]. This included investigating the compounds' absorption efficiency, tissue distribution, metabolic transformations, elimination routes, and potential adverse effects. Computational tools such as SwissADME(http://www.swissadme.ch/index.php) and pkCSM (https://biosig.lab.uq.edu.au/pkcsm/prediction) were employed for predictive evaluations of drug-likeness and bioavailability [37].

Simultaneously, the pharmacodynamic assessment explored how Naringenin and Luteolin interacted with their targets, unveiling the correlation between concentration and therapeutic effects. By integrating these analyses, a holistic understanding of the compounds' behavior was attained, guiding their further development and optimizing safety and efficacy profiles for potential therapeutic applications.

Results and discussion

Geometry optimization

The optimized geometries of Luteolin and Naringerin are depicted in Figures 1 and 2, respectively. Table 1 represents the optimized bond lengths of luteolin and Naringerin calculated using density functional theory with the B3LYP functional and the 6-311*G(d,p) basis set which ensured a rigorous and precise representation of their molecular structures. The figures provide detailed insights into the spatial arrangement of atoms, including bond lengths, angles, and overall geometry, facilitating a comprehensive understanding of the molecules' behaviors and potential applications. The consistent methodology employed in these calculations aligns with the established practices in quantum chemistry for accurate and reliable results. Further analysis of the optimized geometries can unveil structural similarities or differences between

Luteolin and Naringerin, contributing to the broader knowledge of their molecular properties.

Examining molecular interactions is crucial for comprehending how Griseofulvin may engage with nearby molecules, such as solvent molecules or potential binding partners. This understanding holds significant relevance in the realm of drug design and studies, where the ability to predict and optimize interactions is vital for crafting effective pharmaceuticals. In addition, the analysis of vibrational spectra plays a key role in elucidating how the molecule vibrates and moves, offering valuable insights into its dynamic behavior.

Table 1. Bond lengths of Luteolin and Naringerin

Luteolin		**Naringerin**	
Parameter	**Value (A)**	**Parameter**	**Value (A)**
R(1-8)	1.390	R(1-13)	1.466
R(1-9)	1.398	R(1-14)	1.389
R(2-13)	1.338	R(2-14)	1.472
R(2-28)	1.059	R(2-16)	1.368
R(3-11)	1.232	R(3-10)	1.430
R(4-16)	1.361	R(3-39)	0.993
R(4-29)	0.995	R(4-11)	1.423
R(5-19)	1.368	R(4-40)	0.994
R(5-30)	1.000	R(5-12)	1.430
R(6-21)	1.375	R(5-41)	0.983
R(6-31)	0.991	R(6-17)	1.481
R(7-8)	1.408	R(6-19)	1.360
R(7-11)	1.456	R(7-24)	1.342
R(7-13)	1.426	R(7-51)	1.044
R(8-14)	1.389	R(8-22)	1.227
R(9-10)	1.473	R(9-30)	1.371
R(9-12)	1.348	R(9-52)	0.990
R(10-15)	1.408	R(10-11)	1.546
R(10-18)	1.402	R(10-12)	1.542
R(11-12)	1.463	R(10-31)	1.116
R(12-22)	1.091	R(11-13)	1.547
R(13-17)	1.404	R(11-32)	1.116
R(14-16)	1.410	R(12-14)	1.549
R(14-23)	1.086	R(12-33)	1.118
R(15-19)	1.394	R(13-15)	1.514
R(15-24)	1.093	R(13-34)	1.111
R(16-17)	1.401	R(14-35)	1.111
R(17-25)	1.085	R(15-36)	1.100
R(18-20)	1.401	R(15-37)	1.097
R(18-26)	1.092	R(15-38)	1.101
R(19-21)	1.423	R(16-21)	1.403
R(20-21)	1.393	R(16-23)	1.402
R(20-27)	1.088	R(17-18)	1.526
R(3-28)	1.725	R(17-25)	1.504
-	-	R(17-42)	1.116

Table 1. Continued…

Luteolin	Naringerin	Luteolin	Naringerin
-	-	R(18-22)	1.510
-	-	R(18-43)	1.112
-	-	R(18-44)	1.115
-	-	R(19-20)	1.418
-	-	R(19-21)	1.396
-	-	R(20-22)	1.446
-	-	R(20-24)	1.427
-	-	R(21-45)	1.089
-	-	R(23-24)	1.401
-	-	R(23-46)	1.086
-	-	R(25-26)	1.407
-	-	R(25-27)	1.402
-	-	R(26-28)	1.390
-	-	R(26-47)	1.091
-	-	R(27-29)	1.396
-	-	R(27-48)	1.093
-	-	R(28-30)	1.408
-	-	R(28-49)	1.088
-	-	R(29-30)	1.402
-	-	R(29-50)	1.085
-	-	R(8-51)	1.768

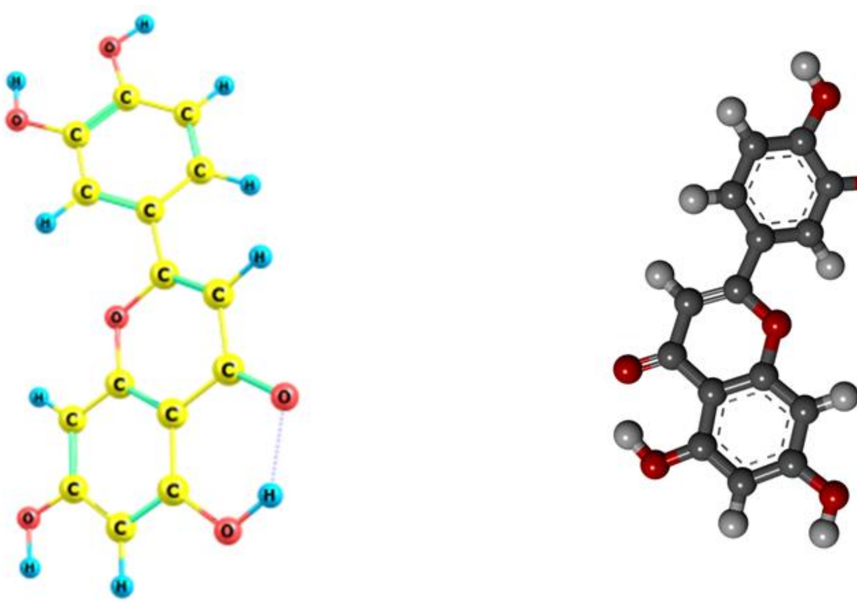

(I) **(ii)**

Figure 1. Optimized geometry of Luteolin.

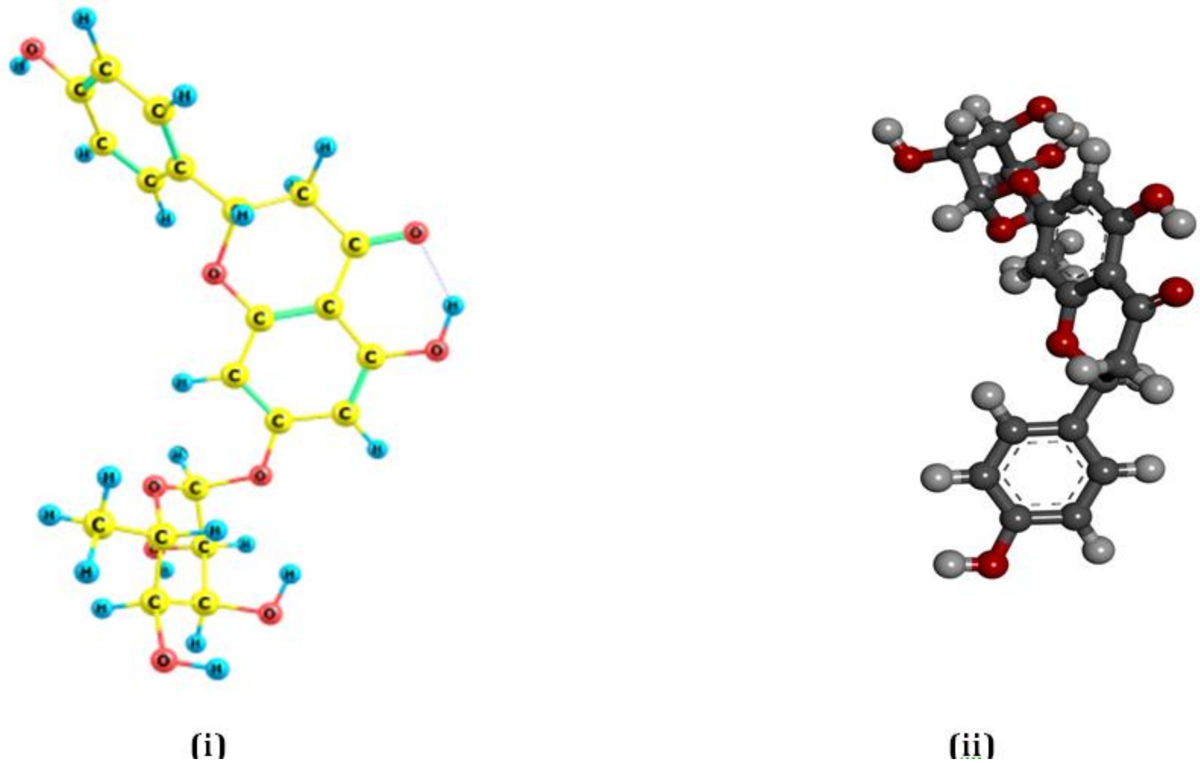

Figure 2. Optimized geometry of Naringerin.

Molecular docking analysis

Molecular docking simulation is a computational method employed in structural biology and drug discovery to predict the preferred orientation of a small molecule ligand when bound to a target protein receptor [46]. Utilizing algorithms based on principles of molecular recognition and thermodynamics, docking software evaluates numerous possible conformations and orientations of the ligand within the binding site of the receptor to estimate the most energetically favorable binding mode. By simulating interactions at the atomic level, docking enables the prediction of binding affinities and potential interactions between molecules, aiding in the design and optimization of novel drug candidates or the investigation of ligand-protein interactions [46].

In Table 2, a distinctive conventional hydrogen bond is observed with PRO30, featuring a precise and directional interaction characterized by a bond length of 2.16553 Å. This shorter distance underscores a well-defined orientation, enhancing the stability of the complex through specific molecular recognition in the binding site. Furthermore, a pi-cation interaction with LYS98, evidenced by a bond length of 4.24384 Å, contributes specificity to the binding. This interaction involves the aromatic system of Luteolin interacting with the positively charged side chain of lysine, and although the bond length is relatively longer, its strength of 4.24384 kcal/mol highlights its significant role in augmenting ligand binding affinity and overall complex stability. The pi-donor hydrogen bond with THR101, featuring a bond length of 3.77135 Å, introduces nuance to the binding, involving both pi electron cloud and hydrogen bonding interactions. Despite a moderate bond length, the combination of these interactions adds robustness to the ligand-protein association. Pi-sigma interactions with LEU35 (bond length: 3.82455 Å) and LYS98 (bond length: 3.91995 Å) emphasize the involvement of aromatic systems in stabilizing the binding complex, providing additional anchoring points that reinforce the structural integrity of the binding site.

Moreover, pi-alkyl interactions with amino acids such as PRO32 (bond length: 5.32236 Å), ARG97 (bond lengths: 5.09429 Å and 4.92643 Å), and LYS98 (bond length: 4.88445 Å) contribute to hydrophobic complementarity between Luteolin and the protein. The varying bond lengths underscore the flexibility and adaptability of these hydrophobic interactions, shaping the overall binding affinity.

Table 2. Protein-Luteolin interactions, amino acid bond distances and binding affinity

Ligand	Protein Code	Binding Affinity (kcal/mol)	Amino acid Residue	Amino acid Bond's Distance (Å)	Types of Interactions
Luteolin	4ZFI	-7.0	PRO30	2.16553	Conventional Hydrogen Bond
			LYS98	4.24384	Pi-Cation
			THR101	3.77135	Pi-Donor Hydrogen Bond
			LEU35	3.82455	Pi-Sigma
			LYS98	3.91995	Pi-Sigma
			PRO32	5.32236	Pi-Alkyl
			ARG97	5.09429	Pi-Alkyl
			LYS98	4.88445	Pi-Alkyl
			PRO32	5.12528	Pi-Alkyl
			ARG97	4.92643	Pi-Alkyl

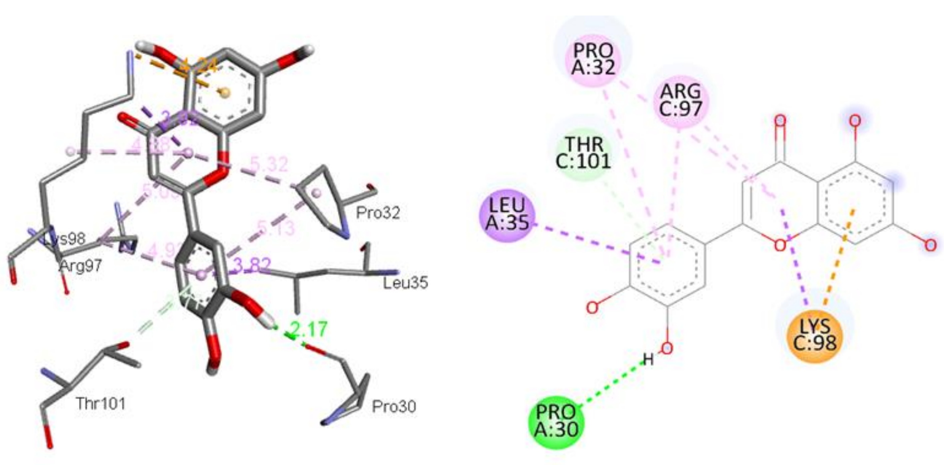

Figure 3. Luteolin-protein interactions

Table 3. Protein-Naringerin interactions, amino acid bond distances and binding affinity

Ligand	Protein Code	Binding Affinity (kcal/mol)	Amino acid Residue	Amino acid Bond's Distance (Å)	Types of Interactions
Naringerin	4ZFI	-7.6	TYR104	2.13172	Conventional Hydrogen Bond
			LEU107	2.72932	Conventional Hydrogen Bond
			LEU107	2.33744	Conventional Hydrogen Bond
			VAL109	3.88949	Pi-Sigma
			TYR104 -	4.59091	Pi-Pi Stacked

Table 3 shows that Naringerin establishes a highly specific and directional interaction with TYR104 and LEU107 through conventional hydrogen bonds, characterized by bond lengths of 2.13172 Å and 2.72932 Å, respectively. These relatively short bond lengths indicate a precise spatial arrangement, underscoring the importance of molecular recognition in the ligand-protein binding site. The formation of multiple hydrogen bonds with distinct amino acids suggests a tailored fit, contributing significantly to the stability of the complex. In addition, the Pi-Sigma interaction with VAL109, featuring a bond length of 3.88949 Å, further enriches the binding profile. This interaction involves the pi electron cloud of Naringerin interacting with the sigma bond of the aromatic system in VAL109, providing an additional layer of stabilization to the complex. The moderate bond length suggests a balanced interaction strength, contributing to the overall adaptability of the ligand-protein association.

Furthermore, the Pi-Pi stacked interaction with TYR104, characterized by a bond length of 4.59091 Å, adds a distinct feature to the binding landscape. This type of interaction involves the stacking of aromatic rings, and the relatively longer bond length implies a more extended interaction. Pi-Pi stacked interactions are known for their contribution to ligand binding stability, and in this context, they enhance the overall structural integrity of the Naringerin-protein complex. The combination of these diverse interactions showcases the adaptability and specificity of Naringerin in engaging with TYR104, LEU107, and VAL109, highlighting the intricate molecular dance that underlies the formation of a stable ligand-protein complex.

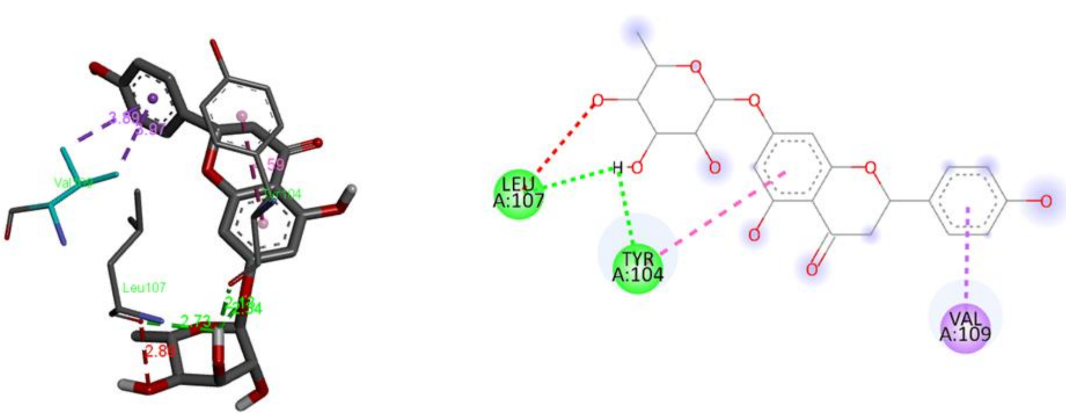

Figure 4. Naringerin-protein interactions

Table 4. HOMO-LUMO energies of Luteolin and Naringerin

Molecule	HOMO Energy(ev)	LUMO Energy(ev)	Energy Difference ΔE (ev)
Luteolin	-9.31480	-1.25391	8.06089
Naringerin	-9.43807	-0.68056	8.75751

Highest occupied molecular orbitals and lower unoccupied molecular orbitals

Table 4 illustrates the electronic characteristics of Luteolin and Naringerin through their Highest Occupied Molecular Orbital (HOMO) and Lowest Unoccupied Molecular Orbital (LUMO) energy levels, demonstrated in Figures 5 and 6. For Luteolin, the HOMO energy level is -9.31480 eV, indicating a stable and electron-rich region. In contrast, the LUMO energy level is -1.25391 eV, suggesting an electron-accepting propensity. The substantial energy difference (ΔE) of 8.06089 eV between the HOMO and LUMO underscores Luteolin's stability and potential for diverse electronic interactions.

The HOMO-LUMO energy gap, also known as the frontier molecular orbital (FMO) gap, plays a crucial role in determining the biological activity and chemical reactivity of a compound. In general, a smaller HOMO-LUMO energy gap indicates higher chemical reactivity and potentially greater biological activity. Similarly, Naringerin exhibits a stable electron-rich region with a HOMO energy level of -9.43807 eV. However, its LUMO energy level is -0.68056 eV, indicating a higher capacity to accept electrons compared to Luteolin. The larger energy difference (ΔE) of 8.75751 eV in Naringerin implies heightened reactivity and broader electronic versatility, suggesting its potential involvement in diverse chemical processes. To sum up, Luteolin and Naringerin display distinct electronic profiles. Luteolin's smaller ΔE indicates a stable yet versatile nature, while Naringerin's larger ΔE suggests heightened reactivity and broader electronic versatility. These electronic characteristics provide valuable insights into the potential roles of these molecules in various chemical contexts.

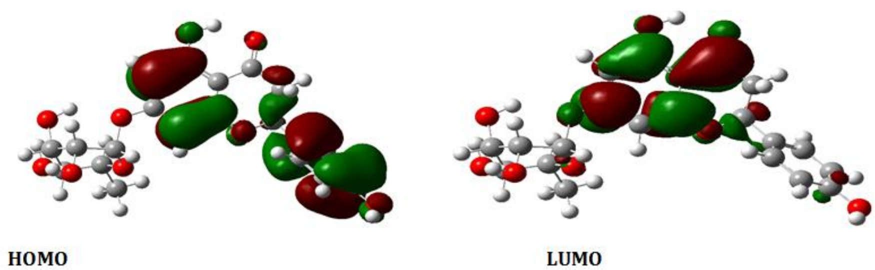

Figure 5. HOMO-LUMO orbitals of Naringerin

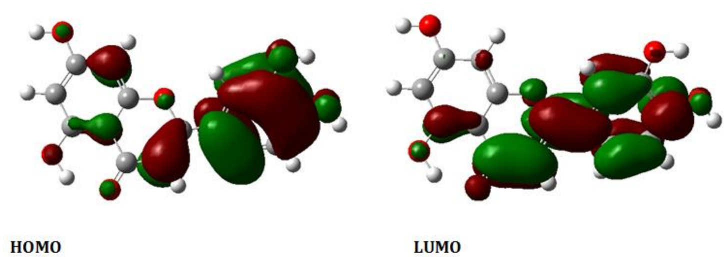

Figure 6. HOMO-LUMO orbitals of Luteolin

Table 5. ADMET properties of Naringerin

Property	**Parameter**	**Predicted value**
Absorption (% Absorbed)	Human Intestinal Absorption	91.31
	Water Solubility	-3.388
Distribution	BBB Permeability	-0.578
	CSN Permeability	-2.215
Metabolism (Cytochrome P450, CYP)	CYP2D6 Substrate	No
	CYP3A4 Substrate	No
	CYP1A2 Inhibitor	Yes
	CYP2C19 Inhibitor	No
	CYP2C9 Inhibitor	No
	CYP2D6 Inhibitor	No
	CYP3A4 Inhibitor	NO
Excretion	Total clearance	0.06
Toxicity	AMES Toxicity	No
	Human Max. tolerated dose (log mg/kg/day)	0.176

ADMET studies

Naringerin, as indicated by its ADMET properties in Table 5, exhibits promising characteristics for therapeutic development. The high predicted human intestinal absorption (91.31%) suggests efficient uptake in the gastrointestinal tract, enhancing potential bioavailability. Despite lower water solubility (-3.388), the overall absorption percentage indicates Naringerin's potential to overcome solubility challenges through alternative mechanisms. This resilience could be particularly advantageous in formulations aimed at improving solubility or optimizing absorption in various delivery methods.

Distribution properties underscore Naringerin's inclination towards peripheral effects, with limited permeability across the Blood-Brain Barrier (BBB) and Central Nervous System (CNS). While this may limit access to the brain, it proves advantageous if the therapeutic target primarily resides in peripheral tissues. Moderate metabolic characteristics, acting as a substrate for CYP1A2, but not major cytochrome P450 enzymes like CYP2D6 and CYP3A4, suggest a manageable metabolic liability. The lack of inhibition of these enzymes further supports a favorable metabolic profile, with potential interactions involving CYP1A2 being a crucial consideration.

Excretion properties suggest a slow total clearance (0.06), indicating a prolonged duration of action and a potentially sustained therapeutic effect. In addition, the absence of AMES toxicity and the low value for the human maximum tolerated dose (0.176 log mg/kg/day) contribute to a favorable safety profile. Taken together, these ADMET characteristics position Naringerin as a promising therapeutic candidate, especially in scenarios where peripheral activity is desirable. Nevertheless, careful consideration of its metabolic interactions, particularly with CYP1A2, is essential when designing treatment regimens involving co-administration with other drugs. From Table 6, Luteolin showcases promising characteristics in its absorption, distribution, metabolism, excretion, and toxicity (ADMET) profile, positioning it as a potential candidate for therapeutic applications.

Table 6. ADMET properties of Luteolin

Property	Parameter	Predicted value
Absorption (% Absorbed)	Human Intestinal Absorption	81.13
	Water Solubility	-3.094
Distribution	BBB Permeability	-0.907
	CSN Permeability	-2.251
Metabolism (Cytochrome P450, CYP)	CYP2D6 Substrate	No
	CYP3A4 Substrate	No
	CYP1A2 Inhibitor	Yes
	CYP2C19 Inhibitor	No
	CYP2C9 Inhibitor	Yes
	CYP2D6 Inhibitor	No
	CYP3A4 Inhibitor	No
Excretion	Total clearance	0.495
Toxicity	AMES Toxicity	No
	Human Max. tolerated dose (log mg/kg/day)	0.499

Its predicted human intestinal absorption (HIA) of 81.13% suggests efficient uptake in the gastrointestinal tract, enhancing its bioavailability and systemic circulation upon administration. However, the challenge lies in its low water solubility (-3.094), which may impact its dissolution in aqueous environments. Strategies to address this solubility challenge could be crucial for optimizing its absorption and overall efficacy.

In terms of distribution, the negative values for Blood-Brain Barrier (BBB) and Central Nervous System (CSN) permeability (-0.907 and -2.251, respectively) indicate limited access to the brain. This points towards a preference for peripheral actions, aligning with its potential applications in conditions where central nervous system effects are not required. The metabolic profile of Luteolin adds complexity, as it is not predicted to be a substrate for major cytochrome P450 enzymes (CYP2D6, CYP3A4), but it does inhibit CYP1A2 and CYP2C9. This suggests a need for cautious co-administration, as interactions with drugs metabolized by these enzymes could affect overall drug metabolism and efficacy.

In terms of excretion, the moderate total clearance value of 0.495 indicates a reasonable rate of elimination. This may influence the duration of therapeutic effects, emphasizing the importance of establishing appropriate dosing intervals for sustained efficacy. The absence of AMES toxicity and the low human maximum tolerated dose (0.499 log mg/kg/day) further contribute to a positive safety profile, suggesting a higher margin of safety in dosing. Overall, Luteolin's unique combination of absorption efficiency, limited central nervous system penetration, complex metabolic interactions, and favorable safety attributes make it a promising candidate for therapeutic development, particularly in applications where peripheral activity is desired.

Conclusion

To sum up, this study has explored the anti-cancer properties of Tigernut-derived compounds, focusing on Naringenin and Luteolin, through molecular docking studies with the 4ZFI protein, a cancer-associated molecular target. The investigation revealed several significant interactions between the flavonoids and the protein, providing insights into potential mechanisms underlying their anti-cancer effects. This computational approach not only expands our understanding of Tigernut compounds' bioactivity, but also highlights the promising role of Naringenin and Luteolin in cancer research. The results of our investigation provide valuable insights into the binding affinities and preferred orientations of Naringenin and Luteolin when interacting with the 4ZFI protein. These interactions signify a potential mechanism through which these compounds may exert their anti-cancer effects, offering a foundation for further exploration and validation. These findings serve as a foundation for future experimental validations and underscore the potential of natural compounds in the development of targeted and effective strategies for cancer prevention and treatment.

Acknowledgements

The authors would like to acknowledge the contributions of all those who have made this work possible. We are grateful for the guidance, support, and expertise of our colleagues, and collaborators. We also appreciate the contributions of our research team, who have worked tirelessly to collect and analyze data, and to write and revise this paper.

Declarations

The authors declare that they have no conflict of interest in this study.

Availability of data and materials

The publisher has the right to make the data Public. All data used in this study will be readily available to the public.

Funding

There is no source of external funding.

Consent for publication

Not Applicable.

Orcid

Deborah Alahira : 0009-0008-3860-4519
John Paul Shinggu : 0009-0005-2216-3155
Bulus Bako : 0009-0001-3946-0712

References

[1]. Babiker E.E., Özcan M.M., Ghafoor K., Al Juhaimi F., Ahmed I.A.M., Almusallam I.A. Bioactive compounds, nutritional and sensory properties of cookies prepared with wheat and tigernut flour, *Food Chemistry*, 2021, **349**:129155 [Crossref], [Google Scholar], [Publisher]

[2]. Pelegrín C.J., Ramos M., Jiménez A., Garrigós M.C. Chemical composition and bioactive antioxidants obtained by microwave-assisted extraction of Cyperus esculentus L. by-products: a valorization approach, *Frontiers in Nutrition*, 2022, **9**:944830 [Crossref], [Google Scholar], [Publisher]

[3]. Tavera-Hernández R., Jiménez-Estrada M., Alvarado-Sansininea J.J., Nieto-Camacho A., López-Muñoz H., Sánchez-Sánchez L., Escobar M.L. Synthesis of chrysin, quercetin and naringin nitroderivatives: antiproliferative, anti-inflammatory and antioxidant activity, *Letters in Drug Design & Discovery*, 2021, **18**:795 [Crossref], [Google Scholar], [Publisher]

[4]. Allen L.N. Commercial determinants of global health, *Handbook of global health*, 2021, 1275 [Crossref], [Google Scholar], [Publisher]

[5]. Xu H., Jia Y., Sun Z., Su J., Liu Q.S., Zhou Q., Jiang G. Environmental pollution, a hidden

culprit for health issues, *Eco-Environment & Health*, 2022, **1**:31 [Crossref], [Google Scholar], [Publisher]

[6]. Fiore M., Oliveri Conti G., Caltabiano R., Buffone A., Zuccarello P., Cormaci L., Cannizzaro M.A., Ferrante M. Role of emerging environmental risk factors in thyroid cancer: a brief review, *International Journal of Environmental Research and Public Health*, 2019, **16**:1185 [Crossref], [Google Scholar], [Publisher]

[7]. Kashyap P., Kumar S., Riar C.S., Jindal N., Baniwal P., Guiné R.P., Correia P.M., Mehra R., Kumar H. Recent advances in Drumstick (Moringa oleifera) leaves bioactive compounds: Composition, health benefits, bioaccessibility, and dietary applications, *Antioxidants*, 2022, **11**:402 [Crossref], [Google Scholar], [Publisher]

[8]. Mottaghipisheh J., Iriti M. Sephadex® LH-20, Isolation, and purification of flavonoids from plant species: A comprehensive review, *Molecules*, 2020, **25**:4146 [Crossref], [Google Scholar], [Publisher]

[9]. Valero-Vello M., Peris-Martínez C., García-Medina J.J., Sanz-González S.M., Ramírez A.I., Fernández-Albarral J.A., Galarreta-Mira D., Zanón-Moreno V., Casaroli-Marano R.P., Pinazo-Duran M.D. Searching for the antioxidant, anti-inflammatory, and neuroprotective potential of natural food and nutritional supplements for ocular health in the mediterranean population, *Foods*, 2021, **10**:1231 [Crossref], [Google Scholar], [Publisher]

[10]. Oyedara O.O., Rufai A.B., Okunlola G.O., Adeyemi F.M. Nutritional and endophytic composition of edible tubers of tiger nut (Cyperus esculentus L.), *Jordan Journal of Biological Sciences*, 2022, **15**:603 [Crossref], [Google Scholar]

[11]. Ushie O., Kendeson A., Longbab B., Ogofotha P., Nongu S., Bako B. Profiling phytochemicals and antimicrobial activities of hexane and acetone crude extracts of sterculia setigera LEAF, *Journal of Chemical Society of Nigeria*, 2022, **47** [Crossref], [Google Scholar], [Publisher]

[12]. Tsado M.J., Ndamitso M.M., Shaba E.Y., Mustapha S., Muhammed S.S., Adamu A.*(IOSR Journal Of Environmental Science, Toxicology And Food Technology*, 2013) [Google Scholar], [Publisher]

[13]. Bako B., Ushie O., Malu S. Lupeol and lauric acid isolated from ethyl acetate stem extract of justicia secunda and their antimicrobial activity, *Journal of Chemical Society of Nigeria*, 2023, **48**:[Crossref], [Google Scholar], [Publisher]

[14]. Shukla D., Rawal R., Jain N. A brief review on plant-derived natural compounds as an anti-cancer agents, *International Journal of Herbal Medicine*, 2018, **6**:28 [Google Scholar], [Publisher]

[15]. Dhanaraj S. A critical review on quercetin bioflavonoid and its derivatives: Scope, synthesis, and biological applications with future prospects, *Arabian Journal of Chemistry*, 2023, **16**:104881 [Crossref], [Google Scholar], [Publisher]

[16]. Ali M.Y., Sina A.A.I., Khandker S.S., Neesa L., Tanvir E., Kabir A., Khalil M.I., Gan S.H. Nutritional composition and bioactive compounds in tomatoes and their impact on human health and disease: A review, *Foods*, 2020, **10**:45 [Crossref], [Google Scholar], [Publisher]

[17]. Bako B. Applications of Justicia secunda extracts in functional foods and natural products: A Review, *Advanced Journal of Chemistry Section B*, 2024, **6**:1 [Crossref], [Google Scholar], [Publisher]

[18]. Prieto-Martínez F.D., López-López E., Juárez-Mercado K.E., medina-franco J.L. computational drug design methods—current and future perspectives, *In Silico Drug Design*,

2019, 19 [Crossref], [Google Scholar], [Publisher]
[19]. Basith S., Cui M., Macalino S.J., Choi S. Expediting the design, discovery and development of anticancer drugs using computational approaches, *Current Medicinal Chemistry*, 2017, **24**:4753 [Crossref], [Google Scholar], [Publisher]
[20]. Saikia S., Bordoloi M. Molecular docking: challenges, advances and its use in drug discovery perspective, *Current Drug Targets*, 2019, **20**:501 [Crossref], [Google Scholar], [Publisher]
[21]. Arjmand B., Hamidpour S.K., Alavi-Moghadam S., Yavari H., Shahbazbadr A., Tavirani M.R., Gilany K., Larijani B. Molecular docking as a therapeutic approach for targeting cancer stem cell metabolic processes, *Frontiers in Pharmacology*, 2022, **13**:768556 [Crossref], [Google Scholar], [Publisher]
[22]. Muhseen Z.T., Li G. Promising terpenes as natural antagonists of cancer: an in-silico approach, *Molecules*, 2019, **25**:155 [Crossref], [Google Scholar], [Publisher]
[23]. Gohain B.B., Gogoi U., Das A., Rajkhowa S. Enhancing cancer drug development with xanthone derivatives: A QSAR approach and comparative molecular docking investigations, *South African Journal of Botany*, 2023, **163**:294 [Crossref], [Google Scholar], [Publisher]
[24]. Ugbe F.A., Shallangwa G.A., Uzairu A., Abdulkadir I. A 2-D QSAR modeling, molecular docking study and design of 2-Arylbenzimidazole derivatives as novel leishmanial inhibitors: a molecular dynamics study, *Advance Journal of Chemistry Section A*, 2023, **6**:50 [Crossref], [Google Scholar], [Publisher]
[25]. Gavas S., Quazi S., Karpiński T.M. Nanoparticles for cancer therapy: current progress and challenges, *Nanoscale Research Letters*, 2021, **16**:173 [Crossref], [Google Scholar], [Publisher]
[26]. Chelliah S.S., Paul E.A.L., Kamarudin M.N.A., Parhar I. Challenges and perspectives of standard therapy and drug development in high-grade gliomas, *Molecules*, 2021, **26**:1169 [Crossref], [Google Scholar], [Publisher]
[27]. Khan J., Sakib S.A., Mahmud S., Khan Z., Islam M.N., Sakib M.A., Emran T.B., Simal-Gandara J. Identification of potential phytochemicals from Citrus limon against main protease of SARS-CoV-2: Molecular docking, molecular dynamic simulations and quantum computations, *Journal of Biomolecular Structure and Dynamics*, 2022, **40**:10741 [Crossref], [Google Scholar], [Publisher]
[28]. Shinggu J.P., Etim E.E., Onen A.I. Quantum chemical studies on C2H2O isomeric species: Astrophysical implications, and comparison of methods, *Communication in Physical Sciences*, 2023, **9** [Google Scholar], [Publisher]
[29]. Frisch, M. J., Trucks, G. W., Schlegel, H. B., Scuseria, G. E., Robb, M. A., Cheeseman, J. R., ... & Fox, D. J. (2009). Gaussian 09, Revision D. 01, Gaussian, Inc., Wallingford CT. *See also: URL: http://www. gaussian. com*.
[30]. Sarikaya E.K., Dereli Ö., Bahceli S. A Comparative study of DFT/B3LYP/6-31G (d, p), RM062X/6-31G (d, p), B3LYP/6-311++ G (d, p) and HSEH1PBE/6-31G (d, p) methods applied to molecular geometry and electronic properties of Cs-C60Cl6 molecule, *Adıyaman University Journal of Science*, 2021, **11**:456 [Crossref], [Google Scholar], [Publisher]
[31]. Shinggu J.P., Etim E.E., Onen A.I. Protonation-induced structural and spectroscopic variations in molecular species: A Computational Study on N2, H2, CO, CS, and PH3, *Communication in Physical Sciences*, 2023, **9** [Google Scholar], [Publisher]
[32]. Surmiak E., Twarda-Clapa A., Zak K.M., Musielak B., Tomala M.D., Kubica K., Grudnik P., Madej M., Jablonski M., Potempa J. A unique Mdm2-binding mode of the 3-pyrrolin-2-one- and 2-furanone-based antagonists of the p53-

Mdm2 interaction, *ACS Chemical Biology*, 2016, **11**:3310 [Crossref], [Google Scholar], [Publisher]

[33]. Trott O., Olson A.J. AutoDock Vina: improving the speed and accuracy of docking with a new scoring function, efficient optimization, and multithreading, *Journal of Computational Chemistry*, 2010, **31**:455 [Crossref], [Google Scholar], [Publisher]

[34]. Rose P.W., Beran B., Bi C., Bluhm W.F., Dimitropoulos D., Goodsell D.S., Prlić A., Quesada M., Quinn G.B., Westbrook J.D. The RCSB Protein Data Bank: redesigned web site and web services, *Nucleic Acids Research*, 2010, **39**:D392 [Crossref], [Google Scholar], [Publisher]

[35]. Norinder U., Bergström C.A. Prediction of ADMET properties, *ChemMedChem: Chemistry Enabling Drug Discovery*, 2006, **1**:920 [Crossref], [Google Scholar], [Publisher]

[36]. Shinggu J.P., Etim E.E., Onen A.I. Isotopic effects on the structure and spectroscopy of thioformaldehyde, dihydrogen and water, *Advanced Journal of Chemistry, Section A*, 2023, **6**:366 [Crossref], [Publisher]

[37]. Pires D.E., Blundell T.L., Ascher D.B. pkCSM: predicting small-molecule pharmacokinetic and toxicity properties using graph-based signatures, *Journal of Medicinal Chemistry*, 2015, **58**:4066 [Crossref], [Google Scholar], [Publisher]

[38]. Surmiak E., Twarda-Clapa A., Zak K.M., Musielak B., Tomala M.D., Kubica K., Grudnik P., Madej M., Jablonski M., Potempa J. A unique Mdm2-binding mode of the 3-pyrrolin-2-one- and 2-furanone-based antagonists of the p53-Mdm2 interaction, *ACS Chemical Biology*, 2016, **11**:3310 [Crossref], [Google Scholar], [Publisher]

[39]. Ghiasi R., Rahimi M. Complex formation of titanocene dichloride anticancer and Al 12N 12 nano-cluster: A quantum chemical investigation of solvent, temperature and pressure effects, *Main Group Chemistry*, 2021, **20**:19 [Crossref], [Google Scholar], [Publisher]

[40]. Ghiasi R., Valizadeh A. Computational investigation of interaction of a cycloplatinated thiosemicarbazone as antitumor and antiparasitic agents with B12N12 nano-cage, *Results in Chemistry*, 2023, **5**:100768 [Crossref], [Google Scholar], [Publisher]

[41]. Strati G.L., Willett J.L., Momany F.A. Ab initio computational study of β-cellobiose conformers using B3LYP/6-311++ G, *Carbohydrate Research*, 2002, **337**:1833 [Crossref], [Google Scholar], [Publisher]

[42]. Srivastava R., Al-Omary F.A., El-Emam A.A., Pathak S.K., Karabacak M., Narayan V., Chand S., Prasad O., Sinha L. A combined experimental and theoretical DFT (B3LYP, CAM-B3LYP and M06-2X) study on electronic structure, hydrogen bonding, solvent effects and spectral features of methyl 1H-indol-5-carboxylate, *Journal of Molecular Structure*, 2017, **1137**:725 [Crossref], [Google Scholar], [Publisher]

[43]. Samuel H., Nweke-Mariazu U., Etim E. Experimental and theoretical approaches for characterizing halogen bonding, *Journal of Appllied Organometallic Chemistry*, 2023, **3**:169 [Crossref], [Publisher]

[44]. Baiz C.R., Błasiak B., Bredenbeck J., Cho M., Choi J.H., Corcelli S.A., Dijkstra A.G., Feng C.J., Garrett-Roe S., Ge N.H. Vibrational spectroscopic map, vibrational spectroscopy, and intermolecular interaction, *Chemical Reviews*, 2020, **120**:7152 [Crossref], [Google Scholar], [Publisher]

[45]. Samuel H.S., Ekpan FM. Revolutionizing drugs administration: Techniques in drug delivery and development, *International Journal of Biochemistry Physiology*, 2023, **8**:000237 [Crossref], [Publisher]

[46]. Milusheva M., Gledacheva V., Stefanova I., Feizi-Dehnayebi M., Mihaylova R., Nedialkov P., Cherneva E., Tumbarski Y., Tsoneva S.,

Todorova M. Synthesis, molecular docking, and biological evaluation of novel anthranilic acid hybrid and its diamides as antispasmodics, *International Journal of Molecular Sciences*, 2023, **24**:13855 [Crossref], [Google Scholar], [Publisher]

How to cite this manuscript: D. Alahira, J.P. Shinggu, B. Bako. Quantum chemical and molecular docking studies of luteolin and naringerin found in tigernut: A study of their anti-cancer properties. *Journal of Medicinal and Nanomaterials Chemistry*, 2024, 6(1), 64-80. DOI: 10.48309/JMNC.2024.1.6